

# Complex Broad Emission Line Profiles of AGN - Geometry of the Broad Line Region

E. Bon<sup>a</sup>, N. Gavrilović<sup>a,b</sup>, G. La Mura<sup>c</sup>, L. Č. Popović<sup>a</sup>

<sup>a</sup>*Astronomical Observatory, Volgina 7, 11060 Belgrade, Serbia*

<sup>b</sup>*Observatoire de Lyon, 9 avenue Charles André, Saint-Genis Laval cedex, F-69561, France ; CNRS, UMR 5574*

<sup>c</sup>*Department of Astronomy, University of Padova, Vicolo dell'Osservatorio, I-35122 Padova, Italy*

---

## Abstract

The Broad Emission Lines (BELs) in spectra of type 1 Active Galactic Nuclei (AGN) can be very complex, indicating a complex Broad Line Region (BLR) geometry. According to the standard unification model one can expect an accretion disk around a supermassive black hole in all AGN. Therefore, a disk geometry is expected in the BLR. However, a small fraction of BELs show double-peaked profiles which indicate the disk geometry. Here, we discuss a two-component model, assuming an emission from the accretion disk and one additional emission from surrounding region. We compared the modeled BELs with observed ones (mostly broad  $H\alpha$  and  $H\beta$  profiles) finding that the model can well describe single-peaked and double-peaked observed broad line profiles.

*Key words:*

Seyfert galaxies, accretion disks, line profiles

---

*Email addresses:* ebon@aob.bg.ac.rs (E. Bon), ngavrilovic@aob.bg.ac.rs (N. Gavrilović), giovanni.lamura@unipd.it (G. La Mura), lpopovic@aob.bg.ac.rs (L. Č. Popović)

## 1. Introduction

The detailed structure of the innermost part of AGN is still an open question. It is widely accepted that the central engine consists of a super massive black hole fueled by an accretion disk. The origin of the broad emission lines, observed in most AGN, is explained by photoionization of dense gas surrounding the nuclei, but the structure and dynamics of the BLR remains unclear. Using Broad Emission Lines (BEL) shape investigations of the BLR, one can constrain the geometry of the material in the BLR (see Popović, 2006).

BELs of AGN show high diversity in their shapes and widths. In some rare cases, where the accretion disk clearly contributes to the BELs, we can investigate the disk properties using a broad, double-peaked, low-ionization lines (Chen & Halpern, 1989; Chen et al., 1989; Eracleous & Halpern, 1994, 2003; Eracleous et. al, 2009). The rotation of the material in the disk results in one blue-shifted and one redshifted peak, while the gravitational redshift produces a displacement of the center of the line and a distortion of the line profile.

Moreover, a number of BELs show shoulders-like profile in the wings of the line, which could be a fingerprint of the accretion disk emission (Popović et al., 2003; Eracleous & Halpern, 2003; Strateva et al., 2003). Beside emission of the disk (or disk-like region) or emission from spiral shock waves within a disk (Chen & Halpern, 1989; Chen et al., 1989), the following geometries may cause substructures in line profiles: i) emission from the oppositely-

directed sides of a bipolar outflow (Zheng et al., 1990, 1991); ii) emission from a spherical system of clouds in randomly inclined Keplerian orbits illuminated anisotropically from the center (Goad & Wanders, 1996); and iii) emission of the binary black hole system (Gaskell, 1983, 1996);

To explain the complex morphology of the observed BEL shapes, different geometrical models have been discussed (see in more details Sulentic et al., 2000). In some cases the BEL profiles can be explained only if two or more kinematically different emission regions are considered (see e.g. Marziani et al., 1993; Romano et al., 1996; Popović et al., 2001, 2002, 2003, 2004; Bon et al., 2006; Ilić et al., 2006; Collin et al., 2006; Hu et al., 2008). In particular, the existence of a Very Broad Line Region (VLBR) with random velocities at 5000-6000 km/s within an Intermediate Line Region (ILR) has also been considered to explain the observed BEL profiles (Corbin & Boroson, 1996; Sulentic et al., 2000; Hu et al., 2008).

Nevertheless, the majority of AGN with BELs have only single peaked lines, but this does not necessarily indicate that the contribution of the disk emission to the BELs profiles is negligible.

In this paper we study the possibility that the flux of the hidden disk emission could be present in single peaked emission line profiles of AGN. With this goal, we applied a simple, two-component model, which assumes that observed BELs can be represented by composition of the emission of the accretion disk and surrounding non-disk isotropic region. For the accretion disk emission, we have used the model proposed by Chen & Halpern (1989), which assumes optically thick and geometrically thin disk, while for the additional emitting region which surrounds the disk, we assumed isotropic

velocity distribution of emitting clouds, which imply that the emission line profiles generated by this region can be described by a Gaussian function. In Section 2 of this paper we describe samples of galaxies where we analyzed the possible accretion disk contribution to the total flux of their broad emission lines. We review the methods of analyzes in Sections 3 and in Section 4 we give results. Finally, in Section 6 we outline our conclusions.

## 2. Data sets

First sample of 12 AGN spectra was observed with the 2.5 m INT on La Palma at 2002 (Popović et al., 2004). For some lines with bad S/N ratio we used HST observations obtained with the Space Telescope Imaging Spectrograph (STIS) on January 2000 (NGC 3516). Details about observation and data reduction can be find in (Bon et al., 2006; Popović et al., 2004) The narrow and satellite lines were cleaned (see e.g. Popović et al., 2002, 2003, 2004).

With the idea to compare our model with real emission line profiles, without fitting, we used the sample of spectra containing 90 broad-line-emitting AGN, which have been collected by La Mura et al. (2007) from the third data release of Sloan Digital Sky Survey (SDSS)<sup>1</sup>. The spectra were already corrected for sky-emission, telluric absorption, the Galactic extinction and redshift (La Mura et al., 2007). Since the interest was to investigate the broad emission line profiles, we subtracted the narrow components of H $\alpha$  and the satellite [NII] lines. The spectral reduction (including subtraction of

---

<sup>1</sup><http://www.sdss.org/dr3>

stellar component) and the way to obtain the broad line profiles are in more details explained in La Mura et al. (2007).

Previously cleaned broad H $\alpha$  profile was normalized, converted from wavelength to velocity scale, using DIPSO software package<sup>2</sup>.

The sample of 90 AGN contained the spectra with different FWHM of broad H $\alpha$  from about 1000 km/s to 7000 km/s, with at least several representatives in every 500 km/s La Mura et al. (see Table 2 in 2007). This covered many different types of broad single-peaked profiles.

### 3. Methods of BEL profile analyzes

We performed several tests to find a possible accretion disk contribution to the total line flux of a single peak broad emission lines.

#### 3.1. Gaussian fit

We used a  $\chi^2$  minimization routine to obtain the best fit. To limit the number of free parameters in the fit, we have set some *a priori* constraints as given in Popović et al. (2003).

In the fitting procedure, we looked for the minimal number of Gaussian components needed to fit the broad component. For the narrow blending lines we have been taking into account the intensity ratio of [OIII] lines (obtained from the atomic values 1:3.03) and the fit of Fe II template for the H $\beta$ . In the case of H $\alpha$  line, for the narrow [NII] lines we assume that their

---

<sup>2</sup><http://www.starlink.rl.ac.uk>

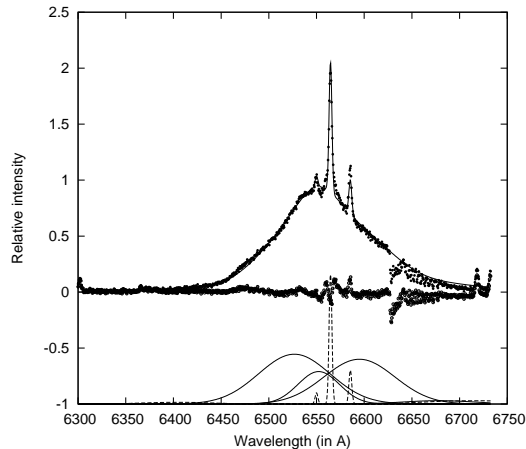


Figure 1: Decomposition of the  $H\alpha$  line of Mrk 841. The dashed lines represent the observations, while the solid lines show the profile obtained by Gaussian decomposition. The Gaussian components are presented at the bottom. The narrow dashed lines correspond to the narrow  $H\alpha$  and  $[NII]$  lines.

intensity ratio is 1:2.96 (see Popović et al., 2003, 2004; Bon et al., 2006). Some examples are presented in Figures 1 and 2.

The results of indicated existence of two kinematic regions, one very broad line region (VBLR), represented by the two shifted Gaussians and one intermediate broad line region (ILR), represented with the central Gaussian component. It was noticed that both shifted components had similar widths, while the central component had similar values to the central components of the other lines (see Fig. 3), what led to idea to introduce the two component model, that consists of the accretion disk (which could describe the wings of the line), and surrounding region with isotropic velocities of clouds (representing the core of the line, that can be described by a Gaussian).

These results encouraged us to test in the same manner the sample of 12 AGN (Popović et al., 2004). After Gaussian decomposition the results

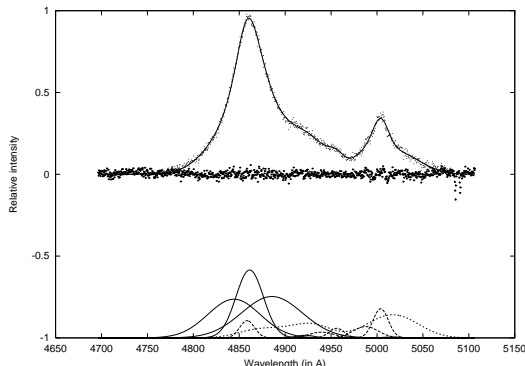


Figure 2: Decomposition of the  $H\beta$  line of 3c 273. The dashed lines represent the observations while the solid lines show the profile obtained by Gaussian decomposition. The Gaussian components are presented at the bottom. The narrow dashed lines correspond to the narrow  $H\beta$ , [OIII] lines and FeII shelf.

showed again two distinct kinematic regions. The results of Gaussian analysis showed that Fe II lines had comparable widths to the central component (see Fig. 3), indicating that they originate in the same region, what was previously shown by Marziani et al. (2003) and recently by Hu et al. (2008).

### 3.2. *Fit with a two-component model*

For the disk emission, we adopted disk model developed by Chen & Halpern (1989). We fitted the profiles with composition of the disk and Gaussian profiles (see Figures 4-6). Starting value of the width of the Gaussian was considered to be the value of the width of the central Gaussian obtained from the fit with three broad Gaussians components, for the same object. All those lines were expected to have a common inclination, since they originate in the same object, so this constrain was taken into account.

Using these results as a starting point, we fitted with the two-component

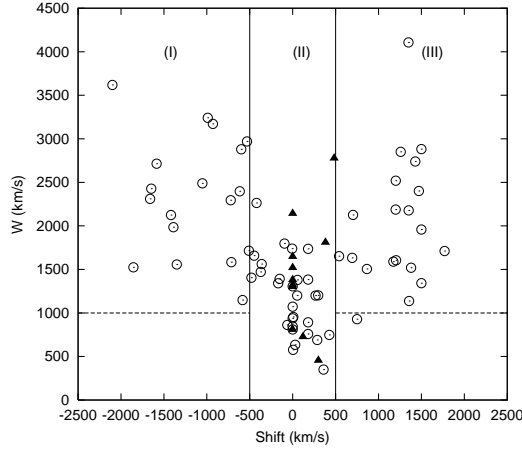


Figure 3: The widths ( $w$ ) as a function of the shifts of the broad Gaussian components obtained for the  $H\alpha$  and  $H\beta$  lines of our sample of AGNs (open circles) and the Fe II template (full triangles) (Popović et al., 2004).

model the profile composed as averaged  $H\alpha$  and  $H\beta$  line of each AGN (see Popović et al., 2004).

The results of the fit are presented in Figs 4-6, and corresponding parameters of two component model are given in Tables 1-3 for 12 AGN. As one can see from Figs 4-6, the line profiles can be well fitted with a two-component model. Depending on the inclination, local broadening and the dimension of the accretion disk, a line from the disk can appear as single or double-peaked.

The parameters obtained by fitting the line profiles are given in the Tables 1-3 for 12 AGN. Here we presented several tests of fitting with two component model. We fixed the emissivity parameter as  $p=3$  (Table 1) and also as  $p=2.5$  (Table 2), with allowing all other parameters to be free. While searching for the maximal inclination of the disk, we obtained values of parameters presented in Table 3. For the parameter that correspond to the



shift of the disk component, there are several possible explanations, like a motion of emitters in elliptical disks (Eracleous et al., 1995), tidal perturbation of the disk around a supermassive black hole by a smaller companion (Eracleous et al., 1995), or some binary black hole configurations in which BLR is dominated by the gravity of one black hole. The orbital motion of two black holes around their center of mass can result in radial velocity shift of the entire BLR (see for example Boroson & Lauer, 2009; Bogdanović et al., 2009). Moreover, one can expect different types of turbulence caused by magnetic field in the accretion disk (see e.g. Turner et al., 2003) that in the case of the line additionally contribute to the line broadening. The magnetic field could produce the effects of the accretion inflow and outflow around the back hole (see. e.g. Ohsuga et al., 2009), that also can partly contribute to the width and shift of a line originated from a small disk cell.

Concerning the disk parameters we can point out the following: (i) The outer radii are very similar in the sample ( $R_{\text{out}} \sim 1500 R_g$ ); (ii) The local random velocities in the disk are different from object to object and they are in the interval from 400 km/s to 1300 km/s. (iii) The inner radii of the emitting disk for all considered objects are in the interval from 300 to 600  $R_g$ , (iv) The obtained inclinations are small ( $5^\circ < i < 15^\circ$ ), and such values of inclinations support the idea that we are in position to more frequently observe the Sy 1 at face-on inclinations.

Concerning the emission of the surrounding region we can point out that: i) the red-shifts are close to the cosmological, they are in the interval of  $\pm 300$  km/s; (ii) the random velocities in this region are also different for different objects, and they are in the interval from 400 to 1600 km/s.

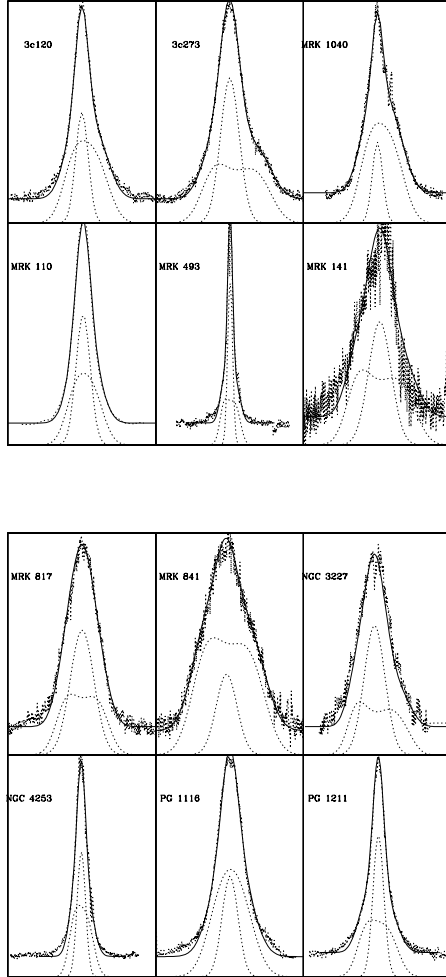


Figure 4: Observed averaged  $H\beta$  and  $H\alpha$  lines of 12 AGNs (dashed lines), fitted with the two-component model (solid lines) which include the emission of an accretion disk and a spherical emission region as a broader or double-peaked contour or a narrower Gaussian, respectively (dashed lines at bottom).

Table 1: The parameters of the disk:  $z_{\text{disk}}$  is the shift and  $\sigma$  is the Gaussian broadening term from disk indicating the random velocity in disk,  $R_{\text{inn}}$  are the inner radii,  $R_{\text{out}}$  are the outer radii. The  $z_G$  and  $W_G$  represent the parameters of the Gaussian component.  $F_s/F_d$  represents the ratio of the relative disk and Gaussian fluxes. The value for parameter of emissivity was fixed as  $p=3$ .

Object	$i$	$z_{\text{disk}}$	$\sigma$ (km/s)	$R_{\text{inn}} (R_g)$	$R_{\text{out}} (R_g)$	$z_G$	$W_G$ (km/s)	$F_s/F_d$
3C 120	10	-300	1060	380	1400	+30	900	0.6
3C 273	14	-30	1140	400	1400	+30	1350	0.8
MRK 1040	8	-250	1050	400	1400	00	750	0.2
MRK 110	7	-320	950	500	1400	+150	1020	0.9
MRK 141	12	-630	1050	300	1100	+200	1620	0.7
MRK 493	5	-480	400	600	1400	+60	360	1.0
MRK 817	12	-450	1050	600	1400	+48	1600	0.95
MRK 841	15	-750	1270	450	1400	-300	1500	0.2
NGC 3227	12	-780	1080	350	1600	+300	1400	0.8
NGC 4253	5	-630	560	500	1500	-30	600	0.7
PG 1116	8	-450	1260	500	1400	+48	1140	0.4
PG 1211	8	-660	830	430	1530	+90	780	0.8

Table 2: The same as in Table 1, but with fixed value for parameter of emissivity as  $p=2.5$

Object	$i$	$z_{\text{disk}}$	$\sigma$ (km/s)	$R_{\text{inn}} (R_g)$	$R_{\text{out}} (R_g)$	$z_G$	$W_G$ (km/s)	$F_s/F_d$
3C 120	14	+300	960	650	2500	+300	960	0.7
3C 273	18	+90	1191	550	1900	+60	1380	0.9
MRK1040	12	0	870	700	2700	00	600	0.2
MRK 110	12	0	890	800	2400	+150	1020	1.4
MRK 141	14	-630	1040	300	2200	+240	1620	0.8
MRK 493	5	-300	280	800	2400	+60	330	0.9
MRK 817	14	-300	1042	600	2400	+48	1690	1.2
MRK 841	23	-300	1270	950	2400	-300	1440	0.3
NGC3227	19	-360	890	800	2600	-300	1500	1.0
NGC4253	8	-150	595	1500	9500	-90	510	0.4
PG 1116	15	0	1480	850	3800	+0	1440	1.0
PG 1211	12	-240	680	730	2530	+90	780	0.9

Table 3: The same as in Table 1, but in search for maximal inclination

Object	$i$	$z_{\text{disk}}$	$\sigma$ (km/s)	$R_{\text{inn}} (R_g)$	$R_{\text{out}} (R_g)$	$z_G$	$W_G$ (km/s)	p	$F_s/F_d$
3C 120	30	+360	745	1650	19000	+60	960	2.2	0.5
3C 273	30	+330	490	1250	15000	+60	1380	2.8	0.9
MRK 1040	27	+300	700	100	17200	00	480	1.3	0.24
MRK 110	30	+210	280	1800	22400	+150	900	2.0	1.2
MRK 141	33	-450	530	1200	1000	+300	1620	2.1	0.8
MRK 493	30	+60	255	10800	124000	+60	270	1.8	0.7
MRK 817	35	0	600	800	14400	+50	1500	1.9	1.0
MRK 841	50	-150	765	1950	27400	-300	1440	2.1	0.8
NGC 3227	34	-300	620	1300	12600	-300	1500	2.1	0.77
NGC 4253	25	-90	215	2500	69500	-30	510	2.0	0.6
PG 1116	30	0	850	950	15800	+90	1440	2.2	0.3
PG 1211	30	0	383	920	15530	+90	780	1.9	0.2

There are indications that local broadening in the disk and in surrounding region could be correlated (see Tables 1-3). It could indicate that those parameters could be linked by the same process, like wind-disk interaction, or something similar.

On the other side, we compared the disk parameters obtained from the two-component model with the ones obtained by fitting the double-peaked line profiles with the disk model only. Eracleous & Halpern (1994) fitted a sample of 12 double peaked AGNs with the disk model. In comparison with their results, our disk parameters are with smaller inclination and also smaller outer radii. Strateva et al. (2003) investigated the spectra of 116 AGNs with double peaked lines using the disk model. and obtained inclinations of the accretion disks smaller than  $50^\circ$ , while inner radii were from  $200 R_g$  to  $800 R_g$  and local turbulent velocities were from 780 km/s to 1800 km/s, that well fitted our estimated values (see Tables 1-3). Comparing those parameters with ones in Tables 1-3, we can conclude that they could be in a good agreement, even though our inclinations were significantly smaller than upper value of those given by the authors. Moreover, for double-peaked lines one can expect a higher inclination, because the value of inclination strongly affects the line width, even for smaller values of emissivity index. For the outer radii, the estimated values were larger than  $2000 R_g$  (Eracleous & Halpern, 1994; Strateva et al., 2003). Our results showed smaller values of outer radii in comparison with those estimated from (Eracleous & Halpern, 1994; Strateva et al., 2003), (see Tables 1-3).

### 3.3. Estimation of the accretion disk contribution to the BELs

Due to a large number of free parameters, we were not able to determine an unique solution of parameters for the best fit (see Figs 3-6). Therefore, we introduced alternative approach to the analysis of the disk contribution to the single peak broad emission lines.

First we set some constrains in the parameter space, and we constructed a grid of simulated line profiles. As a rough approximation, we fixed the width of the central Gaussian component to the 1000 km/s, as mean value obtained from the two component model fit (Bon et al., 2006). As it was shown in Popović et al. (2004), the random velocities in the disk and in the non-disk region were approximately the same, so it was also fixed to the value of 1000 km/s.

The flux ratio of the simulated profiles was given by the parameter  $Q = \frac{F_s}{F_{\text{disk}}}$ , where  $F_s$  is the flux emission from the spherical region and  $F_{\text{disk}}$  is the flux emission from the accretion disk. In the simulations the different values of the parameter  $Q$  have been considered, with the composite profile normalized to unity. The emissivity of the disk as a function of radius,  $r$ , is given by  $\epsilon = \epsilon_0 r^{-p}$ .

We created the grid of simulated BEL profiles with different parameters of the two component model. To reduce free parameters we estimated some constrains. Due to small change in profiles we could fix the following parameters:

- the emissivity of the disk was fixed to  $p=3$ ,
- the Gaussian broadening in the disk was fixed to 1000 km/s,

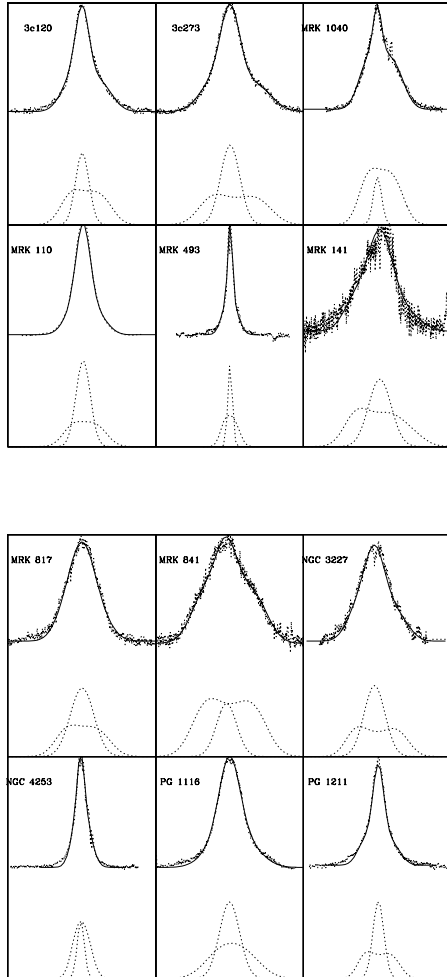


Figure 5: The same as in Fig. 4, but for  $p=2.5$ .



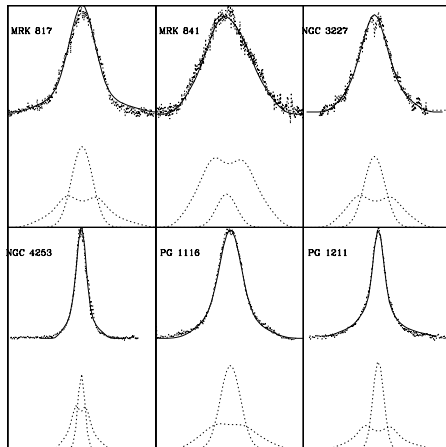
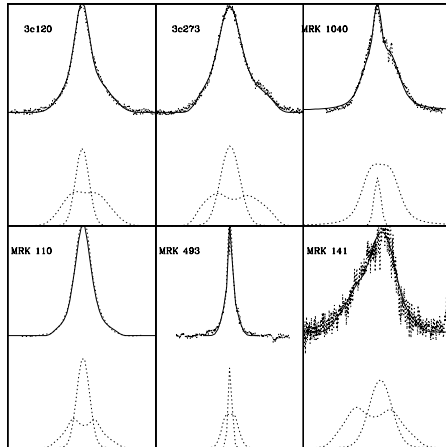


Figure 6: The same as in Fig. 4, but for maximal value of inclination, and with constraints that  $i > 25$ .

- the random velocities of the isotropic component was also fixed to 1000 km/s,
- there were no big differences in shape of the profiles if the outer radius was higher then several thousands  $R_g$ ,
- as a mean value of results obtained from the fit, we fixed the size of inner and outer radius for the first sample of 12 AGN  $R_{inn}=400 R_g$  and  $R_{out}=3000 R_g$ , while for the second sample of 90 SDSS AGN, these parameters were fixed by averaging the disk size obtained from the fitting of the double-peaked lines in the work of Eracleous & Halpern (2003), so we fixed the inner radius to be  $R_{inn}=600 R_g$ , and the outer  $R_{out}=4000 R_g$ .

It was noticed that for the change of the shape of BEL profiles, variation of inclination and the flux ratio played dominant role, so the grid of models was finally reduced only to these two parameters. Simulated spectra were compared to the spectra from different samples.

First the profiles were normalized to the same intensity. We noticed that the variation of the emissivity parameter could be neglected since normalized profiles showed very small change in shape (see Bon et al., 2009; Bon, 2008). For that reason, this parameter was fixed to the value  $p=3$ .

For each line profile, the full widths at 10%, 20%, 30% of maximum intensity were measured, and compared after being normalized to full width at half maximum, which was introduced through coefficients  $k_j$  ( $j = 10, 20, 30$ ) as  $k_{10} = w_{10\%}/w_{50\%}$ ,  $k_{20} = w_{20\%}/w_{50\%}$  and  $k_{30} = w_{30\%}/w_{50\%}$ .

Fixing the inner and outer radius to an averaged value, obtained from

the study of BELs with double-peaked lines (Eracleous & Halpern, 2003), we estimated the values of  $i$  and  $Q$  for all analyzed galaxies.

For the first sample, the inner radius of the disk was chosen to be  $R_{inn} = 400 R_G$ , as the mean value of this parameter in the previous fittings (Bon, 2008). For the outer radius, the chosen value was  $R_{out} = 3000 R_G$ , although the mean value of the outer radius for the sample was about 30000 (Bon et al., 2006), since the variation of this parameter, after values of several thousand gravitational radii, did not show significant influence to the shape of the line (especially if the line is noisy).

#### 4. Results

In order to estimate possible disk presence in the single peaked broad emission lines of AGN, we applied several methods.

From the Gaussian analysis we could conclude that two distinct kinematic regions might be present in the BELs. The central Gaussian component indicated the existence of the emission from the region with intermediate velocities (ILR), while in the wings two shifted broad Gaussians indicated possible presence of disk-like emission (VBLR). The results for the widths of the emission lines of Fe II template showed that these lines probably originate in the ILR (see Figures 1-3).

From the fit with two component model where one component represents the emission from the accretion disk (mostly affects the wings of the emission line), and another from the surrounding region with isotropic velocity distribution of the emitters (that contribute to the core of the line), we can conclude:

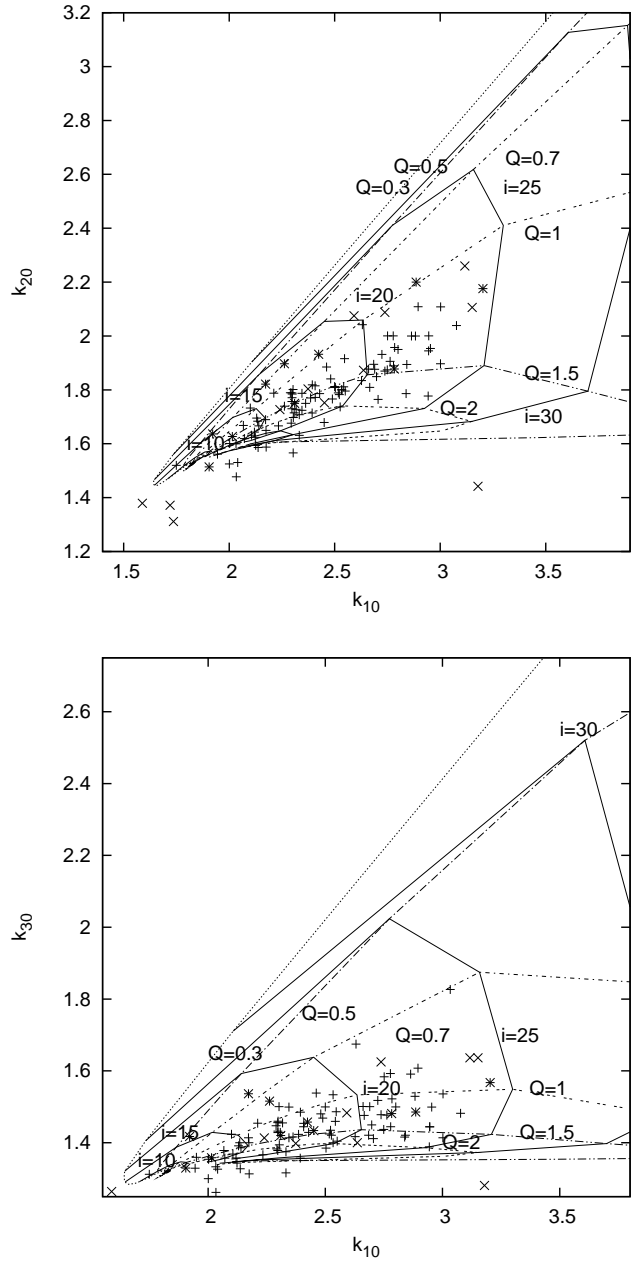


Figure 7: The measured width ratios (crosses-sample of 90 SDSS, asterisks-sample of 12  $H_\alpha$ , x signs-sample of 12  $H_\beta$ ) and simulated values (dashed lines) from the two-component model for the different contribution of the disk emission to the total line flux ( $Q=0.3, 0.5, 0.7, 1, 1.5$  and 2) and different inclinations are considered (solid iso lines presented  $i = 10, 15, 20, 25$  and 30 degrees, respectively).20

- two component model can well fit the profiles of broad emission lines of our samples, but it is very hard to determine the disk parameters, because of the large number of the free parameters (see Figs 4-6),
- random velocities in the surrounding region with isotropic velocities are similar to random velocities in the disk, what implies that these two regions could be connected through some process (for example through the wind of the accretion disk),
- the values of the parameters indicate that the inclinations are smaller than  $50^\circ$ , and the dimensions of the disk could be from several hundred  $R_g$  for the inner radius, to several hundred thousands  $R_g$  for the outer radius.

After comparing the measurements of  $k_i$  for the sample, with the measurements of the simulated profiles, we could derive the estimates of  $i$  and  $Q$ . As the result, we found that the most of the measured points were between  $0.5 < Q < 1.5$ , and  $10^\circ < i < 25^\circ$  (see Fig. 7). The results showed a consistence between estimations of  $i$  and  $Q$  for both  $H\alpha$  and  $H\beta$ , with very small discrepancies (see Table 1 in Bon, 2008).

After this analysis, we tested this method to the larger sample of 90 AGN (see Bon et al., 2009). The measurements were performed in the same way as with 12 AGN, with the difference that we compared it to the simulated spectra with the disk dimensions of  $R_{inn} = 600 R_g$  and  $R_{out} = 4000 R_g$  (averaging the disk size obtained from the fitting of the double-peaked lines in the work of (Eracleous & Halpern, 2003)). With this sample we measured only  $H\alpha$  lines. As it could be seen in Fig. 7, most of the measurements are

located within  $1 < Q < 2$ , and  $10^\circ < i < 25^\circ$  (see Bon et al., 2009).

## 5. Conclusions

In this paper we outline our recent investigation about the presence of the disk emission in single peaked BELs.

We carried out the following analyzes: i) fitting of single peaked BELs with Gaussians and with two component model, and ii) comparing line parameters of a sample with simulated profiles.

From our investigations we can conclude that there could be a high probability that the disk emission flux might be present in the single peaked emission line profiles. In principle, the contribution of the disk emission to the total flux of the single peaked BELs is in most cases smaller than 50%. Also, we found that the disk inclinations were mainly smaller than  $i < 25^\circ$ . Such small inclinations and large discrepancies from simulated profiles for higher inclinations should be discussed in the context of unified model, i.e. possible disk orientation to the torus or partial obscuration by the torus.

## Acknowledgments

The work was supported by the Ministry of Science and Technology of Serbia through the project 146002: “Astrophysical spectroscopy of extragalactic objects“. We would like to thank to Jack W. Sulentic, Paola Marziani, Michael Eracleous and Martin Gaskell for many helpful discussions and comments.

## References

- Bogdanović, T., Eracleous, M., Sigurdsson, S., 2009, *ApJ*, **697**, 288
- Bon, E., Popović, L. Č., Ilić, D., Mediavilla, E.G., 2006, *NewAstRev*, **50**, 716.
- Bon, E., 2008, *Serb. Astron. J.* **177**, 9.
- Bon, E., Popović, L. Č., Gavrilović, N., La Mura, G., Mediavilla, E.G., (2009), *MNRAS*, *accepted*.
- Boroson, T. A.; Lauer, T. R., (2009), *Nature*, **458**, 53.
- Chen, K. & Halpern, J. P. (1989), *ApJ*, **344**, 115.
- Chen, K., Halpern, J. P., Filippenko, A. V., 1989, *ApJ* **339**, 742.
- Corbin, M. R. & Boroson, T. A. 1996, *ApJS*, **107**, 69.
- Collin, S., Kawaguchi, T., Peterson, B. M., Vestergaard, M. 2006, *A&AS*, **456**, 75
- Eracleous, M. & Halpern, J. P., 1994, *ApJS*, **90**, 1,.
- Eracleous, M., Livio, M., Halpern, J. P., Storchi-Bergmann, T., 1995, *ApJ*, **438**, 610.
- Eracleous, M. & Halpern, J. P., 2003, *ApJ*, **599**, 886,.
- Eracleous M. et. al, 2009, *NewAstRev* this issue.
- Gaskell, C. M. 1983, Proc. 24th Liege Intern. Ap. Colloquium, Univ. de Liege, Liege, **473**.

- Gaskell, C. M. 1996, *ApJL*, **464**, 107.
- Goad, M. & Wanders, I. 1996, *ApJ*, **469**, 113.
- Hu, C. , Wang, J. M., Chen, Y. M., Bian W. H., Xue S. J., 2008, *ApJ*, 683L,  
115H
- Ilić, D., Popović, L.Č., Bon, E. Mediavilla, E. G., Chavushyan, V. H. 2006,  
*MNRAS*, **371**, 1610
- La Mura, G., Popović, L. Č., Ciroi, S., Rafanelli, P., Ilić, D. 2007, *ApJ*, **671**,  
104.
- Marziani, P.; Sulentic, J. W.; Calvani, M.; Perez, E.; Moles, M.; Penston, M.  
V., 1993, *ApJ*, **410**, 56
- Marziani, P.; Sulentic, J. W.; Zamanov R. , Calvani M. , Dultzin-Hacyan,  
D., Bachev, R., and Zwitter, T., 2003, *ApJ*, **145**, 199.
- Ohsuga K., Mineshige, S., Mori, M., Kato, Y., 2009, *PASJ*, **61**, 7.
- Popović, L. Č., 2006, *Serb. Astron. J.* **344**, 115.
- Popović, L. Č., Mediavilla, E.G., Kubičela, A., Jovanović, P., 2002, *A&A*,  
**390**, 473.
- Popović, L. Č., Mediavilla, E.G., Bon, E., Ilić, D., 2004, *A&A*, **423**, 909.
- Popović, L. Č., Mediavilla, E.G., Bon, E., Stanić, N., Kubičela, A., 2003,  
*ApJ*, **599**, 185.
- Popović, L. Č., Stanić, N., Kubičela, A., Bon, E. 2001, *A&A*, **367**, 780.



- Romano, P, Zwitter, T., Calvani, M., Sulentic, J. 1996, *MNRAS*, **279**, 165.
- Strateva, I. V. , Strauss, M. A., Hao, L., Schlegel, D. J., Hall, P. B., Gunn, J. E., Li, L.-H., Ivezić, Ž., Richards, G. T., Zakamska, N. L., Voges, W., Anderson, S. F., Lupton, R. H., Schneider, D. P., Brinkmann, J., Nichol, R. C. 2003, *ApJ* **126**, 1720.
- Sulentic, J. W., Marziani, P. & Dultzin-Hacyan, D. 2000, *ARAA*, **38**, 521.
- Turner, N. J., Stone, J. M., Krolik, J. H., Sano, T., 2003, *ApJ*, **953**, 992.
- Zheng, W., Binette, L., Sulentic, J.W. 1990, *ApJ*, **365**, 115.
- Zheng, W., Veilleux, S., Grandi, S.A., 1991, *ApJ*, **381**, 418.